RSC Advances

ROYAL SOCIETY OF CHEMISTRY

www.rsc.org/advances

Jones-Ray effect on the organization of lysozyme in the presence of $NaNO_3$ at air/water interface: Is it a cause or consequence?

Maheshkumar Jaganathan[a], Aruna Dhathathreyan[a]*, Chellappan Selvaraju[b], Reinhard Miller[c]

[a]Biophysics lab., CSIR-CLRI, Adyar, Chennai 600020, India

[b]National Centre for Ultrafast Processes, University of Madras, Taramani Campus, Chennai 600113, India

[c]Max-Planck-Institut fuer Kolloid- und Grenzflaechenforschung, D-14424 Golm/Potsdam, Germany

Author for correspondence

Aruna Dhathathreyan

Chief Scientist

Biophysics Lab., CSIR-CLRI

Adyar, Chennai 600020, India

Email aruna@clri.res.in

Abstract

The study reports on the anomalous aggregation and enhanced viscosity of lysozyme (Lyz) in the presence of low concentration of sodium nitrate at air/buffer interface. For salt concentrations of about 10 mM of $NaNO_3$, the interactions seem to be electrostatic in origin possibly due to the anisotropy of charge distribution on the protein and its correlation with high-complementarity non-electrostatic interactions resulting in sudden increase in viscosity values. In the presence of low concentrations of the electrolyte, a thick viscoelastic protein film is created due to local amorphous aggregation, while native Lyz adsorbs in a fragile monolayer film without changing its secondary structural features. On increasing concentration beyond 10 mM, the protein behaves almost like pure buffer without showing any surface activity or aggregation and is highly stable at the interface. For the first time, the rheological changes here confirm the Jones-Ray effect due to the synergy between $NaNO_3$ (~10 mM) and the protein whereas earlier reports on this effect have dealt only with pure electrolytes-water interactions. Our experimental studies indicate that with the appropriate choice of solution conditions and specific electrolyte concentration, one can either drive the protein to form amorphous aggregates which can result in protein crystallization or enhance protein stability for long time periods by preventing aggregation through self-association.

Introduction

It is well known that the structure of a protein is dependent on both the amino-acid sequence as well as its solvent environment.[1] Often, non-native conformations of the proteins occur through drastic changes in their tertiary structure that can be attributed partially to unfolding and exposure of hydrophobic interior of the protein to the solvent medium. Under right conditions, such unfolded protein species may associate and form a reticulated three-dimensional network that extends throughout the entire medium, entrapping the solvent. An understanding of such aggregated gelation processes in proteins is of importance to understand the mechanisms involved in the folding processes and also in food products.[2-5]

The study of aggregation phenomena in proteins is also of great importance, owing to their implication into a number of systemic and neurodegenerative diseases.[6,7] Theories and experiments dealing with protein aggregation suggest that aggregates are formed from partially folded intermediates.[8] Such supramolecular assemblies of peptides and proteins have also been used to design new and useful biomaterials.[9-11] Adsorption of such assemblies to solid or liquid substrates result in refolding,[12] cooperative effects,[13] surface aggregation,[14] orientational, positional and importantly conformational transitions.[15, 16] This reorganization in proteins often accompanied by desolvation at the backbone level leads to hydrophobic collapse which seems to initiate insoluble fibrillar assemblies. In most of the destabilization processes of the protein, α-helix – β sheet transition seems to be a crucial factor which also provides a link between the structure of the protein and its response to mechanical deformation.[17, 18]

The biological milieu of the protein is organic – aqueous in nature and often controlled by charge distributions as well as polar – non-polar forces and therefore, a study of protein folding and degree of intermolecular association in such environments is relevant in protein structural research. In this work, we present a rheological approach on lysozyme (Lyz) a globular protein, at room temperature in the presence of sodium nitrate. Normally this enzyme displays Newtonian behavior in aqueous solution.[19] Owing to its relatively simple structure and reduced size, hen egg white lysozyme is one of the best suited models to study protein unfolding and aggregation. The solution behavior of lysozyme is also well understood in terms of its interaction with salt ions.[20-22]

However, the folding routes and delays in achieving the necessary conformation for the enzyme to still retain its activity could be dependent on the near solvent environment which in turn can alter the local viscosity or charge or polar – non-polar distributions of the protein. The Hofmeister series, a qualitative list of ions based on their hydration and precipitation of protein according to their polarities and sizes are divided into chaotropes and kosmotropes based on their hydration forces. The typical order of the anionic series is $H_2PO_4^-$> $HCOO^-$> Cl^-> NO_3^-> ClO_4^-> SCN^-. Specific ion effects occurring in many biological and chemical phenomena, such as protein folding, enzyme activity, bacterial growth, transport across membranes, and colloidal assembly have been the subject of study in the recent years.[23-25]

While protein unfolding and enzyme deactivation have begun to be understood as a function of effects manifested through the Hofmeister series, the effects of salt type on protein aggregation are not understood, despite recent success at capturing and

modeling their kinetics.[26-27] Rubin et al. have studied salt induced aggregation in lysozyme through a protein interaction parameter and have demonstrated ion specific aggregation trends in the protein.[19] Stabilization of Lyz using high and medium charge density ions have been studied by Bye and Falconer and in their work they have shown that there are three stages of stabilization and each stage is clearly identified by the free energy change arising through the interaction of the ions with the proteins which itself is dependent on the concentration of the ions used.[28] The effects of different sugars, solvents, ions and cosolutes on the thermodynamic stability of lysozyme have been investigated in depth. These agents are all capable of stabilizing or destabilizing the folded state of a protein.[29-33]

In the present work rheological response of Lyz in the presence of sodium nitrate has been undertaken and the influence of this electrolyte on the dilational rheological parameters and the changes in interfacial activity of the protein has been studied. Further based on these responses the conformational stability as well as transitions have been analyzed using dynamic fluorescence and circular dichroic spectroscopy. While solution viscosity, one of the important thermodynamic parameters, characterizes the solution, the intrinsic viscosity of protein in solution can sensitively reflect protein conformation.[34]

Surface viscoelasticity is known to play a key role in slowing down or preventing droplet coalescence. Coalescence is a process that reduces the interfacial area, thus, if a film is present, it will either be compressed or the molecules will be forced out of the interface. Although there have been a number of research groups working on the relation between surface rheology and bulk rheology, the rheological behavior of protein

films is still an area that is not fully understood from either the experimental or modeling points of view.

In this regard, using the oscillating drop method, the dilational viscosity of protein-surfactant mixtures have been studied by Miller et al.[35, 36] Lakshmanan et.al. in their work on Hofmeister effects and its role on coupled water regulation in BSA have shown the strong influence of the electrolytes on the rheological behavior.[37] Sankaranarayanan et al. have demonstrated the correlation between dilational viscosity, elasticity, and the conformational changes of the Myoglobin films at the interface.[38]

In the present study, it is assumed that for small deformations of the liquid drop containing the protein, the mechanical response of the surface layer will be linear with the applied strain. The experiments presented here are in this linear response regime. There are two fundamental modes of mechanical deformation for a surface: shear (at constant area), and compression (at constant shape). In this study the response of Lyz at air/solution interface in the presence of $NaNO_3$ at constant shape or compression mode has been analyzed.

Experimental

Materials

Hen egg white Lysozyme and the salts were all sourced from Sigma-Aldrich, USA. Lyz has been dialyzed with HPLC grade water and the concentration of each lysozyme stock was measured and adjusted using the absorbance at 280 nm. The electrolytes obtained from Sigma, USA were 99.9% pure. Roasting of all the salts used have been

carried out and measurements have been made before and after roasting and the difference in surface tension of the solutions (negligible compared to pure water) have been measured and are within permissible errors.

Concentration of the solution was fixed at 1 μM in Phosphate buffer (10 mM) at pH=7.5. The final concentrations of the electrolyte with the buffer have been fixed for the total ionic strengths ranging from 1 mM to 100 mM.

Drop Profile Analysis Tensiometry-Dilational Rheology

Freshly prepared solutions of the protein for each measurement with and without the $NaNO_3$ have been used and equilibrium surface tension values as a function of time have been first measured. The volume of the sample PTFE trough was 10 ml. Before each measurement lysozyme samples have been prepared in ultrapure water, and the protein concentration adjusted spectrophotometrically using the extinction coefficient ε of the molecule at 280 nm (ε=37750 $M^{-1}cm^{-1}$). 25 μL of this stock solution has been injected slowly into the subphase of the pre-equilibrated buffer, giving a final protein concentration of 1 μM of the protein.

The dilational rheological parameters of the solutions have been measured with the profile analysis tensiometer PAT-1 (SINTERFACE Technologies, Germany) with an accuracy of 0.1 mN/m and thermostated at a temperature of 22 °C. The solution drops have been formed at the tip of a PTFE capillary immersed into a cuvette filled with a water-saturated atmosphere. After reaching the adsorption equilibrium, the solution drop has been subjected to harmonic oscillations with frequencies (f) 0.01 - 0.2 Hz in order to study the dilatational elasticity. Accuracy in elasticity and viscosity values are 1 mN/m

and 1 mNs/m respectively. Each measurement has been repeated at least three times, and the averages of these three measurements are presented in this study. The surface tension (surface pressure, $\pi = \gamma_{buffer} - \gamma_{lyz}$) oscillations have been measured parallely. The elasticity modulus has been determined from the amplitude ratio of the oscillations of surface tension and surface area. In every experiment, after equilibrium values have been reached, the protein films skimmed from the surface have been characterized using fluorescence and circular dichroism (CD) spectroscopy.

Shear Interfacial Rheology-Storage and Loss Modulus

Rheological measurements have been carried out using a Paar Physica MCR 301 rheometer equipped with cone plate geometry (25 mm radius and 18 cone angle). Oscillatory, transient and static experiments have been run. All experiments have been performed at 21±0.05 °C (Peltier system). Application of a constant shear stress onto systems for a given time interval, followed by removal of stress and monitoring of system strain response as a function of time has been used to measure storage (*G*') and loss (*G*'') moduli for the protein and protein with increasing $NaNO_3$ concentration. 10 mins. have been given as waiting time before start of the rheological measurements. This is a large enough period for a complete formation of a film at air/buffer interface.

Picosecond-Time-Resolved Fluorescence Spectroscopy

Fluorescence lifetime measurements of samples have been carried out in a picosecond-time-correlated single-photon-counting (TCSPC) spectrometer. The excitation source is the tunable Ti-sapphire laser (Spectra Physics, United States). The laser pulse (pulse width of 2 ps and repetition rate of 4 MHz) has been derived from the frequency-

doubled output (532 nm) of mode-locked laser (Spectra Physics, United States). The picosecond standard tuning range is 720-850 nm. The sample has been excited by the laser pulse at 280 nm and emission monitored at right angles to the excitation path. The first photon was detected by the microchannel plate photomultiplier tube (MCP-PMT) (Hamamatsu-C 4878). When the first excitation pulse occurred, a synchronization pulse triggered the charging of the capacitor in the time to amplitude convertor (TAC) through the discriminator. The voltage on the capacitor increased linearly until a stop timing pulse was detected on repeating the start-stop cycle, and a histogram representative of the fluorescence decay obtained has been further analyzed using the IBH (Glasgow, United Kingdom) software[39] and fitted. The values obtained have been corrected to three decimal places with the corresponding standard deviations.

Circular Dichroic Spectroscopy

Circular dichroism measurements have been performed on samples using a spectropolarimeter, model J-815 (Jasco, Japan), with 150 W Xe arc lamp. The instrument has been equipped with a Neslab RTE-110 temperature controller (Neslab Instruments, United States) and calibrated with a standard solution of (+)-10-camphorsulfonic acid. Quartz cuvettes of 0.1 cm path length (Hellma, United States) have been used in the far-UV (190-240 nm) region with a scanning speed of 50 nm/min. Photomultiplier voltage did not exceed 600 V in the spectral regions measured. Data accumulation has been made 3 times and the average spectra have been taken for processing after baseline-correction with the buffer spectrum. All the measurements have been performed at room temperature and the data expressed in mean residue ellipticity. The secondary structural features have been fitted using Dichroweb.[40]

Results and Discussion

Ion Mediated Protein Reorganization at the Air/Water Interface

The change in surface tension γ_{lyz} of pure protein and the protein with different concentration of $NaNO_3$ as a function of time is shown in Fig. 1(a). Pure lysozyme undergoes a lag phase which is seen also with the protein+$NaNO_3$ mixed systems. Such lag phase is indicative of local rearrangement of the hydrodynamically coupled water around the protein competing with the electrolyte - water interactions. The lag phase has been reported for the enzyme in earlier work and the values of surface tension are also agreeable with the reported results.[41, 42] The final surface tension values at equilibrium start to move towards that of pure protein (at [$NaNO_3$] = 50 mM) and at 100 mM the values are nearly that of pure water. However this lag phase disappears at very high concentrations of the electrolyte suggesting that the large concentration of Na^+ and NO_3^- ions interacting with the H^+ and OH^- slows down the diffusion coefficients possibly due to changes in the local viscosity. This lag phase can also be seen as a real effect in Fig. 1(b) which shows the minimum time needed for the rise in surface tension (time lag) for the given concentrations of $NaNO_3$. This initial steady lag phase can possibly be due to the reorganization of protein at the air/buffer interface.

Fig 1(c) presents the plot of surface pressure and steady state fluorescence anisotropy as against [$NaNO_3$]. The plot seems to suggest that there is a preferential exclusion of $NaNO_3$ from protein surfaces due to their increasing ability to exert cohesive forces on water. Anisotropy is a measure of the average molecular orientation

of the protein, while the surface pressure is indicative of cohesive interactions between the molecules expressed at a micro scale. The cohesive effect is reflected in the increasing surface pressure (π) as more $NaNO_3$ is added resulting in the depletion of air/water interface. It follows that, if a solute increases the surface tension of water, more work is required to increase the surface area of the cavity occupied by the protein in the solution.

Fig. 1(c) also particularly supports existence of the Jones-Ray effect. Jones and Ray reported a minimum in the surface tension for 13 strong salts at low concentration of the order of 1 mM. This original observation now called as the 'Jones-Ray effect' has remained controversial and has neither been proven nor disproved unambiguously.[43, 44] However many recent experimental studies using second harmonic generation (SHG) have shown that the Jones-Ray effect could truly exist for different anions due to their propensity to adsorb at the air/water interface leading to decrease in surface tension.[45] Our study demonstrates that the 'Jones-Ray' effect could arise predominantly from a viscoelastic effect due to the competing protein-water and $NaNO_3$–water interactions and not just due to concentration gradient in electrolytes at the air/buffer interface as suggested so far. Moreover this effect seems to be strongly dynamic in nature as seen from our rheological studies.

Significance of Viscosity and Elasticity at the Interface

The dependencies of the dilational rheological indicators: elasticity and viscosity for a constant concentration of Lyz with varying concentration of $NaNO_3$ are plotted as a function of the excitation frequency and for a fixed oscillation amplitude of 1 % and are

shown in Fig. 2(a). The elasticity of the protein in the presence of $NaNO_3$ increases nearly 3 fold with increasing concentration of the electrolyte while the viscosity drops by almost an order to nearly that of water. For all samples, the moduli have been measured even at low frequencies, and some dependency was found till about 0.05 HZ after which no frequency dependence was found. As the concentration of the electrolyte increases, the protein solution possibly starts to resemble water where hydrated protein-cation or anion interactions compete with that of hydrated protein-protein interactions. At lower concentrations, the protein sustained through transient (non-covalent) multiple contacts, displays a spatial network structure of great flexibility, able to stand considerable deformation, as indicated by the wide extent of the linear viscoelastic region observed.

Several experimental studies have shown that in proteins a hydration shell of water exists. In general, molecules of water in protein solutions may be classified into three (i) buried internal, (ii) ordered water on protein surface and (iii) disordered.[46, 47] The first category of water molecules which are likely to fill the cavities inside a protein play an important role in the process of folding of a protein and in its overall stability. On the protein surface, an ordered network of water molecules attached through hydrogen bonds to the atoms of oxygen and nitrogen, or to the polar groups of the amino acid residues are extensively found. Water molecules from these two groups are considered as an integral to the protein. Disordered water molecules, are classified under the bulk water. Krienke in his work on the influence of molecular structure on the conductivity of sodium nitrate in water has shown that the dielectric constants decrease for the higher $NaNO_3$ concentrations.[48, 49] Thus as $NaNO_3$ concentration increases beyond 50 mM, the

solution should behave almost like pure buffer. In order to confirm this, a plot of surface tension against time has been analyzed. This is also in agreement with the MDS results of Thomas et al. on solution-air interface of aqueous $NaNO_3$ where they have shown that NO_3^- resides mostly below the surface for a wide range of concentrations.[50] Even when the ions approach solutions at or near a surface they remain fairly uncoordinated.

Viscoelastic Behavior of Lyz-Electrolyte Mixtures

Fig. 2(b) shows the plot of G' and G" as a function of time for the protein and protein with $NaNO_3$ from shear rheological measurements. It is seen that in all the plots, at least two regions are distinguishable. The storage modulus G′ decreases with time for all the samples while G" stays constant initially. A pronounceable linear viscoelastic regime seen from the constant G' region is found only with the protein+$NaNO_3$ and this disappears rapidly in the pure protein. The high values of G' values for $NaNO_3$ concentrations beyond 10 mM are strongly suggestive of the change in local viscosity and thus also the overall distribution of the protein segments at the air/buffer interface.

This study attempts to understand the transient changes in the protein-water and protein-$NaNO_3$ networks and also the dynamic nature of the protein at air/solution interface. Thus every experimental point measured pertains to instantaneous changes than changes over a long period of time. This is relevant in the context of viscoelastic properties of the protein that is most likely form 'weak gel-like' structures which tend to be dynamic in nature. In general, rheological studies of biopolymers have been shown to have competing processes of intermolecular (protein-protein) versus intramolecular (entanglement arising from protein conformational changes) interactions determining

the nature of G' and G''.[51] Classically, this is determined by the instantaneous surface density of hydrated protein versus protein-$NaNO_3$ at the air/solution interface. However, in our study, protein-$NaNO_3$ networks seem to override the protein-protein interactions forming a 'weak gel-like' structure that is viscoelastic. Thus the local interfacial changes seen in this study seem to be violating the classical G'/G'' relation.

Generally the electrolyte can disturb the water near the surface of the protein in two ways: either through electrostatic interaction or by displacement of the water molecules. An electrostatic perturbation refers to the effect of the leading edge of the double layer reaching the first layer of solution; a displacement refers to an associated ion pair or molecular species, such as NO_3^- complexing with water near the surface. It is suggested that the nature of the solution dictates which mechanism is more significant. Thus for low concentrations, the NO_3^- ion possibly binds loosely with the hydrodynamically coupled water. But as concentration of the electrolyte increases, NO_3^- interacts with the H^+ and behaves like an ion pair.

Hard Protein Behavior of Lyz

In order to study the Lyz films at the interface the skimmed films from the air/solution interface have been subjected to various characterization techniques. Lyz is a well characterized protein and the emission from tyrosine residues is negligible. There are 6 tryptophan residues in Lyz (28, 62, 63, 108, 111, and 123) with Trp-62, Trp-63, and Trp-108 located in the active site. Steady state fluorescence studies have shown that most of the Lyz emission is due to Trp-62 and Trp-108.

The steady state results indicated that the 6 tryptophans are not independent emitters and the existence of non-radiative energy transfer from Trp-108 to Trp-62 has been suggested. The analysis of the data for double exponential decays yielded the values shown in Table I. In the data, one can analyze emission from Trp-62, Trp-108, and the composite emission from the Trps (residues 28, 63, 111, and 123). Trp 63 and 123 do not participate in any fluorescence. The presence in their neighborhood of disulphide linkages (Cys(76)-Cys(94) and Cys(6)-Cys(127) respectively) induces a quenching of their emission.[52] This observation is reinforced also by Nishimoto et al.[53]. At 345 nm the contributions of Trp62 and Trp108 are almost equal and can been estimated from the work of Nishimoto et al to be nearly 92 % of the total emission of the protein.[53,54] The remaining contributions are from Trp28 and Trp111, which have a maximum emission in the blue side of the spectrum. As the emission spectrum of the fully denatured protein is known to exhibit a red shift of about 14 nm,[55] which is not evidenced for any of our samples, a denaturation of the adsorbed protein is very unlikely. This result is in accordance with the known “hard protein behavior” of the lysozyme.

Spectroscopic Investigations-From Molecular to Macroscopic Properties

The τ_1 and τ_2 values for the pure protein are 1.795 $\pm$0.012 and 0.215$\pm$0.017 ns for the emission from Trp 62 and the composite emission from the 3 Trps respectively. The decrease of the average lifetime with increasing concentration of sodium nitrate (Table 1) is in agreement with a modification of the polarity of the surrounding medium of the tryptophans observed at 345 nm. This can be correlated to the confinement of the protein due to the highly conserved network of the nitrate ions around the polar and

charged residues of the protein. The decay of the fluorescence emission of the pure Lyz and Lyz+NO_3 has been presented in Fig. 3.

Fig. 4 shows the CD spectra of the pure protein and with varying concentration of $NaNO_3$. The plots show clearly the gradual shift in the secondary structure as $NaNO_3$ increases. After a concentration of 50 mM the conformation seems to return to total helical state. Table 2 presents the secondary structural changes from CD spectra, showing clearly the transition from helix to β sheet through an intermediate β turn state suggesting that increasing $NaNO_3$ alters the protein conformation. However, on further increasing the concentration of $NaNO_3$ to 100 mM, a complete reversal to helicity is observed (secondary structural population of nearly 99.9 % helix). Depending on the local charge distribution changes that take place around the protein, within the main macroscopic states of folded and unfolded forms of the molecule, small local motions can take place that ultimately leads to a progressive change of conformation with increasing electrolyte concentration. This is similar to the two-state model of the unfolding process, since local rearrangements probably only slightly alter the distribution of secondary structures of the protein without compromising the activity.[56-58]

This study has tried to address the macroscopic properties of aqueous Lyz solution and its molecular properties at air−buffer interfaces. For that purpose we have applied a unique combination of interfacial rheology measurements like dilational and shear rheological parameters with structural information from fluorescence and CD spectra.

In general, the surface tension data, dilational rheological parameters as well as the secondary structural changes establish that the protein in the presence of small concentrations of $NaNO_3$ and the surface tension at air/buffer interface is relatively insensitive. However after a threshold concentration of 10 mM the surface tensions as well as other parameters are strongly altered which in turn is reflected in the secondary structural changes of the protein. Control experiments on the protein alone did not show any drastic changes in the conformation.

Conclusion

This work confirms the Jones-Ray effect for low concentrations of $NaNO_3$ even in the presence of Lyz at air/buffer interface, arising from enhanced interfacial properties of the protein. Such dynamic interfacial properties of the protein in the presence of electrolytes could play an important role in understanding protein crystallization, aggregation induced denaturation etc.[59]

The effect seen here is possibly due to the preference of NO_3^- ion to reside at the interface which synergizes the surface activity of the protein leading to faster and efficient adsorption to the air–buffer interface. This is in agreement with the recent study by Marocco and Michelson who have demonstrated increased presence of the nitrate ion at or near the interface in frozen aqueous solutions.[60]

The results in this study show that in the presence of the electrolyte, a thick and strongly viscoelastic protein film is created due to local aggregation, while native Lyz adsorbs in a fragile monolayer film. This strongly suggests that the air/water interface could be considered as a useful tool to reveal very subtle differences between

differently solvated protein molecules. This ability of a protein to form organized states at the interface at concentrations far below those for bulk aggregation may have implications in protein crystallization at interfaces.

Acknowledgements

MJ would like to thank the Department of Science and Technology (DST), Govt. of India for the INSPIRE Senior Research Fellowship. The authors acknowledge DST, Govt. of India for project grants.

References

1. R. H. Pain, (Eds.), Mechanisms of Protein Folding, 2nd ed., Oxford University Press, Oxford, 2000.

2. A. Dan, G. Gochev, J. Kragel, E. V. Aksenenko, V. B. Fainerman and R. Miller, *Curr. Opin. Colloid & Interface Sci.,* 2013, **18**, 302.

3. G. J. O'Neill, T. Egan, J. C. Jacquier, M. O'Sullivana and E. D. O'Riordan, *Food Chem.,* 2014, **160**, 46.

4. H. P. Lim, B. T. Tey and E. S. Chan, *J Controlled Rel.,* 2014, **186**, 11.

5. C. D. Munialo, A. H. Martin, E. van der Linden and H. H. J. de Jongh, *J. Agri. Food Chem.*, 2014, **62**, 2418.

6. A. M. Morris, A. W. Murielle and R. G. Finke, *Biochim. Biophys. Acta*, 2009, **1794**, 375.

7. M. Calamai, F. Chiti and C. M. Dobson, *Biophys. J.,* 2005, **89**, 4201.

8. A. Dong, B. Kendrick, L. Kreilgard, J. Matsuura, M. C. Manning and J. F. Carpenter, *Arch. Biochem. Biophys.,* 1997, **347**, 213.

9. M. Fukuto, R. K. Heilmann, P. S. Pershan, S. M. Yu, J. A. Griffiths and D. A. Tirrell, *J. Chem. Phys.,* 1999, **111**, 9761.

10. H. Rapaport, G. Möller, C. M. Knobler, T. R. Jensen, K. Kjaer, L. Leiserowitz and D. A. Tirrell, *J. Am. Chem. Soc.,* 2002, 124, 9342.

11. A. Dhathathreyan and B. U. Nair, *J. Phys. Chem. B,* 2010, **114**, 16650.

12. C. Messerschmidt, S. Svenson, W. Stocker and J. -H. Fuhrhop, *Langmuir*, 2000, **16**, 7445.

13. C. L. McGuiness, G. A. Diehl, D. Blasini, D. -M. Smilgies, M. Zhu, N. Samarth, T. Weidner, N. Ballav, M. Zharnikov and D. L. Allara, *ACS Nano,* 2010, **4**, 3447.

14. T. R. Tosteson, R. Revuelta, B. R. Zaidi, S. H. Imam and R. F. Bard, *J. Colloid Int. Sci.,* 1985, **104**, 60.

15. H. Rapaport, I. Kuzmenko, M. Berfeld, K. Kjaer, J. Als-Nielsen, R. Popovits-Biro, I. Weissbuch, M. Lahav and L. Leiserowitz, *J. Phys. Chem. B,* 2000, **104**, 1399.

16. T. Jaworek, D. Neher, G. Wagner, R. H. Wieringa and A. J. Schouten, *Science,* 1998, **279**, 57.

17. J. V. Edwards, A. D. French, T. Jacks, K. Rajasekaran, pH-directed self assembling helical peptide conformation, in: K. Rajasekaran, J.W. Cary, J.M. Jaynes, E. Montesinos (Ed.), Small Wonders: Peptides for Disease Control, *ACS Symposium Series*1095, American Chemical Society: Washington, DC, 2012; p. 203.

18. K. Sankaranarayanan, B. Sreedhar, B. U. Nair and A. Dhathathreyan, *J. Phys. Chem. B, 2013,* **117**, 1234.

19. J. Rubin, A. S. Miguel, A. S. Bommarius and S. H. Behrens, *J. Phys. Chem. B*, 2010, **114**, 4383.

20. J. M. Broering and A. S. Bommarius, *J. Phys. Chem. B,* 2005, **109**, 20612.

21. J. M. Broering and A. S. Bommarius, *J. Phys. Chem. B*, 2008, **112**, 12768.

22. P. Jungwirth and D. Tobias, *J. Chem. Rev.,* 2006, **106**, 1259.

23. W. Kunz, Specific Ion Effects; World Scientific Publishing Company: Singapore, 2009.

24. W. Kunz, P. L. Nostro and B. W. Ninham, *Curr. Opin. Colloid Interface Sci.,* 2004, **9**, 1.

25. M. C. Gurau, S. -M. Lim, E. T. Castellana, F. Albertorio, S. Kataoka and P. S. Cremer, *J. Am. Chem. Soc.*, 2004, **126**, 10522.

26. J. M. Andrews and C. J. Roberts, *Biochemistry,* 2007, **46**, 7558.

27. C. J. Roberts, *Biotechnol. Bioeng.,* 2007, **98**, 927.

28. J. W. Bye and R. J. Falconer, *J. Phys. Chem. B*, 2014, **118**, 4282.

29. M. A. da Silva and E. P. G. Areas, *Biophys. Chem.*, 2002, **99,** 129.

30. S. James and J. J. McManus, *J. Phys. Chem. B*, 2012, **116**, 10182.

31. T. Kamiyama, M. Morita and T. Kimura, *J. Chem. Eng. Data,* 2004, **49**, 1350.

32. F. Cardinaux, E. Zaccarelli, A. Stradner, S. Bucciarelli, B. Farago, S. U. Egelhaaf, F. Sciortino and P. Schurtenberger, *J. Phys. Chem. B,* 2011, **115**, 7227.

33. S. E. Hill, T. Miti, T. Richmond and M. Muschol, *PLoS ONE,* 2011, **6**, e18171.

34. C. Tanford, K. Kawahara and S. Lapanje, *J. Am. Chem. Soc.,*1989, **89**, 729.

35. R. Miller, M. E. Leser, M. Michel and V. B. Fainerman, *J. Phys. Chem. B*, 2005, **109**, 13327.

36. E. V. Aksenenko, V. I. Kovalchuk, V. B. Fainerman and R. Miller, *Adv. Colloid Interface Sci.*, 2006, **122**, 57.

37. M. Lakshmanan, A. Dhathathreyan and R. Miller, *Colloids and Surf. A: Physicochem. Eng. Aspects,* 2008, ***324***, 194.

38. S. Kamatchi, A. Dhathathreyan, J. Kragel and R. Miller, *J. Phys. Chem. B,* 2012, **116**, 895.

39. V. Karunakaran, P. Ramamurthy, T. Josephrajan and V. T. Ramakrishnan, *Spectrochim. Acta, Part A,* 2002, **58**, 1443.

40. L. Whitemore and B. Wallace, *Nucleic Acids Res.*, 2004, **32**, W668.

41. J. A. deFeijter and J. Benjamins, Adsorption Kinetics of Protein at the Air Water Interface; Royal Society of Chemistry: London, 1987.

42. S. Xu and S. Damodaran, *Langmuir*, 1992, **8**, 2021.

43. A. I. Rusanov and E. A. Faktor, *Russ. Chem. ReV.,* 1974, **43**, 933.

44. P. B. Petersen and R. J. Saykally, *J. Amer. Chem. Soc.,* 2005, **127**, 15446.

45. K. T. Nguyen, A. V. Nguyen and G. M. Evans, *Phys. Chem. Chem. Phys.,* 2014, **16**, 24661.

46. T. V. Chalikian, M. Totrov, R. Abagyan and K. J. Breslauer, *J. Mol. Biol.,* 1996, **260**, 588.

47. P. J. Steinbach and B. R. Brooks, *Proc. Natl. Acad. Sci. U.S.A.,* 1993, **90**, 9135.

48. H. Krienke, *Condensed Matter Phys.,* 2013, **16**, 43006: 1‑12.

49. J. Barthel, R. Buchner and M. Muensterer, *Chemistry Data Series,* **Vol. XII**, Part 2. Dechema, Frankfurt/M, 1995.

50. J. L. Thomas, M. Roeselova, L. X. Dang and D. J. Tobias, *J. Phys. Chem. A,* 2007, **111**, 3091.

51. D. R. Picout and S. B. Ross-Murphy, *The Scientific World J.*, 2003, **3**, 105.

52. R. W. Cowgill, *Biochim. Biophys. Acta*, 1967, **140**, 37.

53. E. Nishimoto, S. Yamashita, N. Yamasaki and T. Imoto, *Biosci. Biotechnol. Biochem.,* 1999, **63**, 329.

54. E. Nishimoto, S. Yamashita, A. G. Szabo and T. Imoto, *Biochemistry*, 1998, **37**, 5599.

55. R. McGuire and I. Feldman, *Biopolymers*, 1975, **14**, 1095.

56. J. Gosline, M. Lillie, E. Carrington, P. Guerrette, C. Ortlepp and K. Savage, *Phil. Trans. R. Soc. Lond. B,* 2002, **357**, 121.

57. S. Ciliberti, P. De Los Rios and F. Piazza, *Phys. Rev. Lett.,* 2006, **96**, 19810.

58. S. Reuveni, R. Granek and J. Klafter, *Phys. Rev. Lett.*, 2008, **100**, 208101.

59. Y. J. Zhang and P. S. Cremer, *Curr. Opin. Chem. Biol.*, 2006, **10**, 658.

60. H. A. Marrocco and R .H. R. Michelsen, *J. Phys. Chem. B*, 2014, **118**, 14929.

Figure Captions

Fig. 1(a) Plot of Surface Tension vs. time of Lyz (●) and Lyz with $NaNO_3$ at different concentrations as follows: 1 mM (○), 5 mM (▽), 10 mM (◆), 50 mM (□), 100 mM (▲) of $NaNO_3$.

Fig. 1(b) Time Lag of Surface tension of Lyz against $NaNO_3$ concentrations.

Fig. 1(c) Surface Pressure vs. Fluorescence Anisotropy plots against $NaNO_3$ concentrations. Blue line shows the fitted curve showing Jones-Ray effect.

Fig. 2(a) Viscous and Elastic components of the dilational viscoelasticity vs. area perturbation frequency at air-water interface.

Fig. 2(b) Plots of storage (G') and loss (G") modulus as a function of time for the protein and protein with $NaNO_3$.

Fig. 3. Time-resolved fluorescence decay plots of Lyz and Lyz+$NaNO_3$ mixtures.

Fig. 4. CD spectra of Lyz (inset) and Lyz+$NaNO_3$ mixtures.

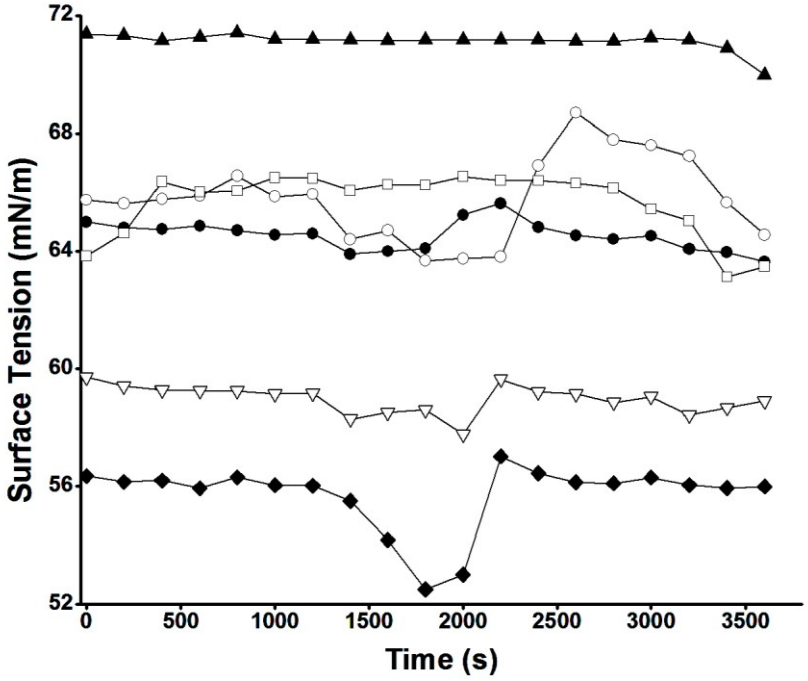

Fig. 1(a)

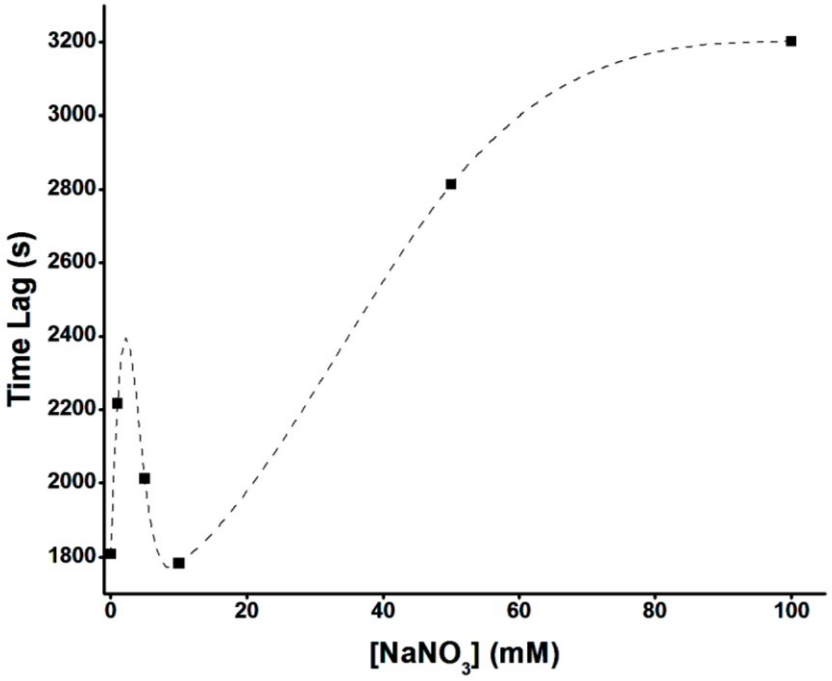

Fig. 1(b)

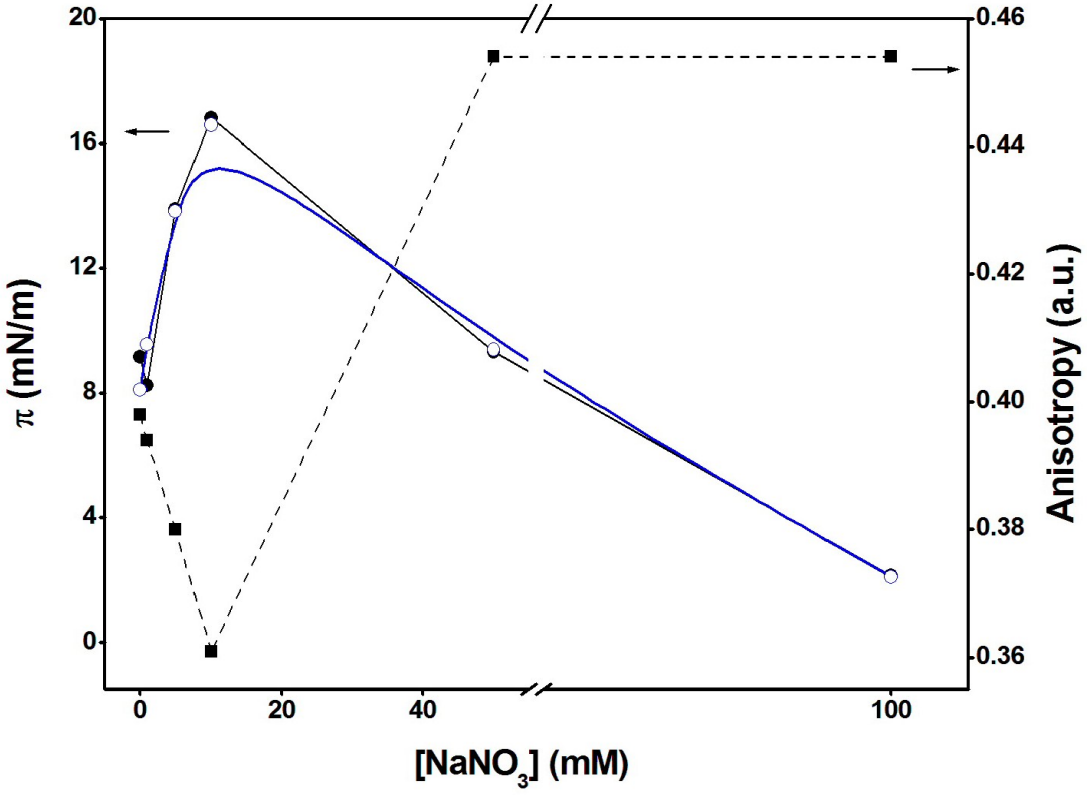

Fig. 1(c)

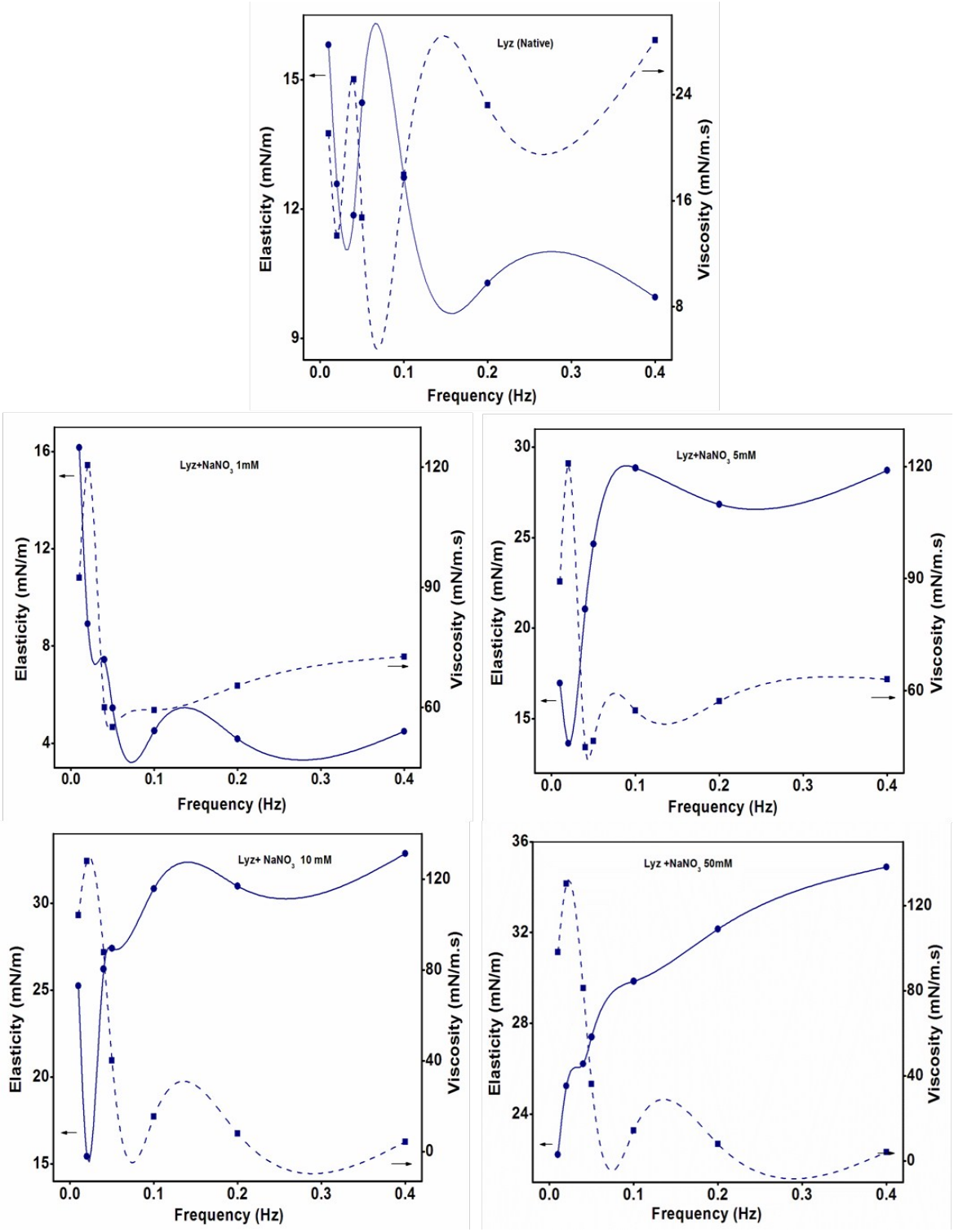

Fig. 2(a).

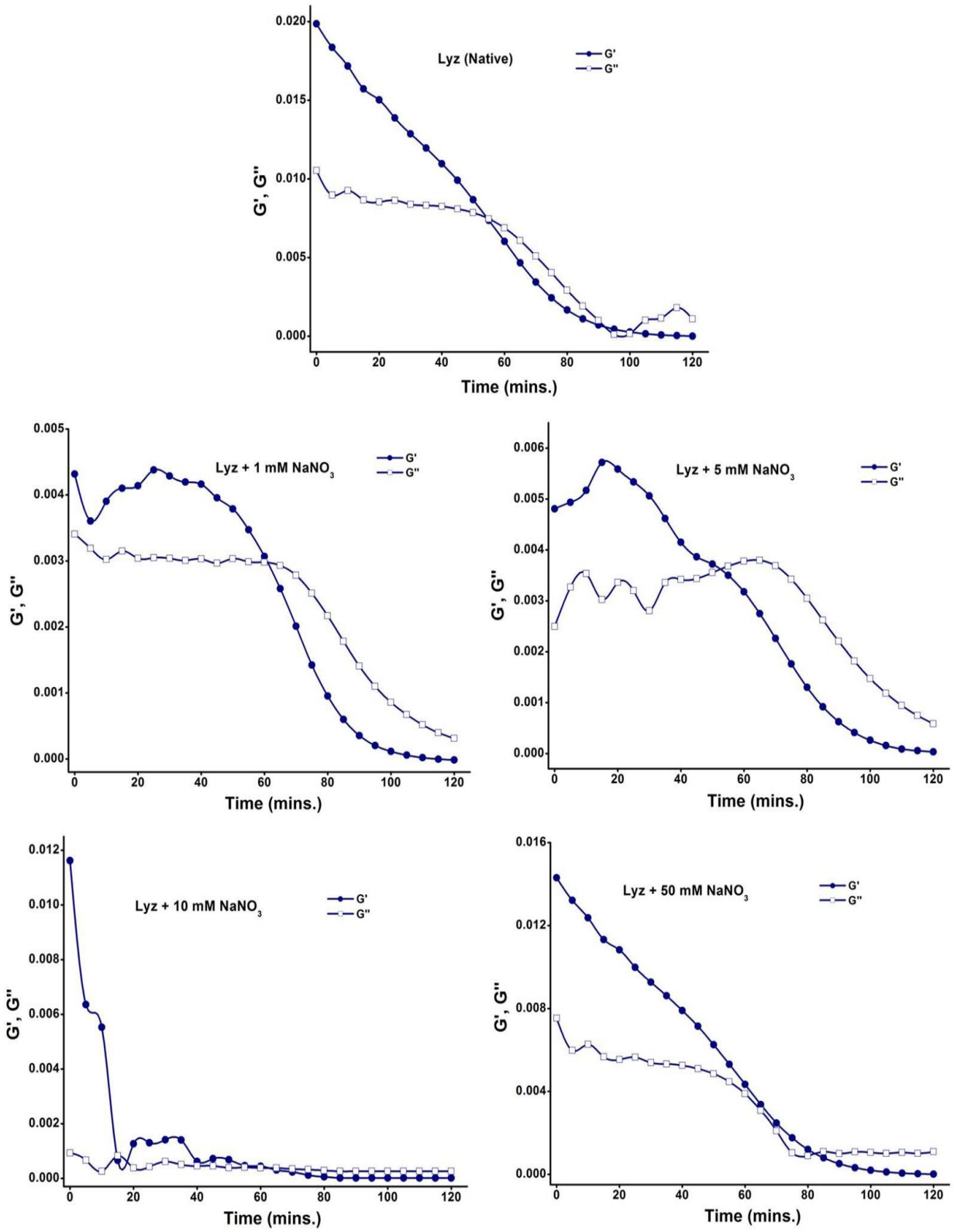

Fig. 2(b)

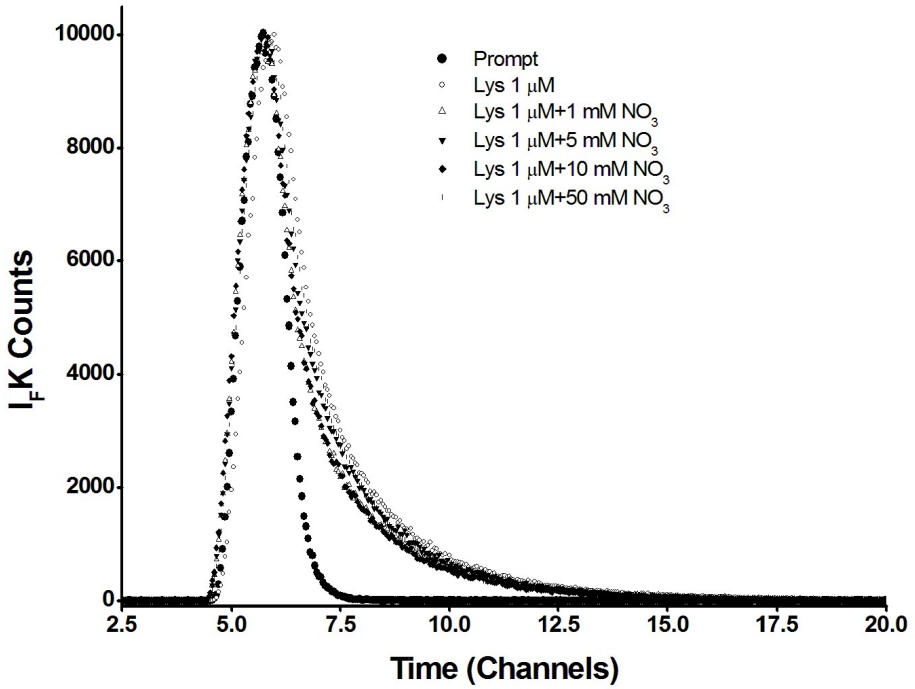

Fig. 3.

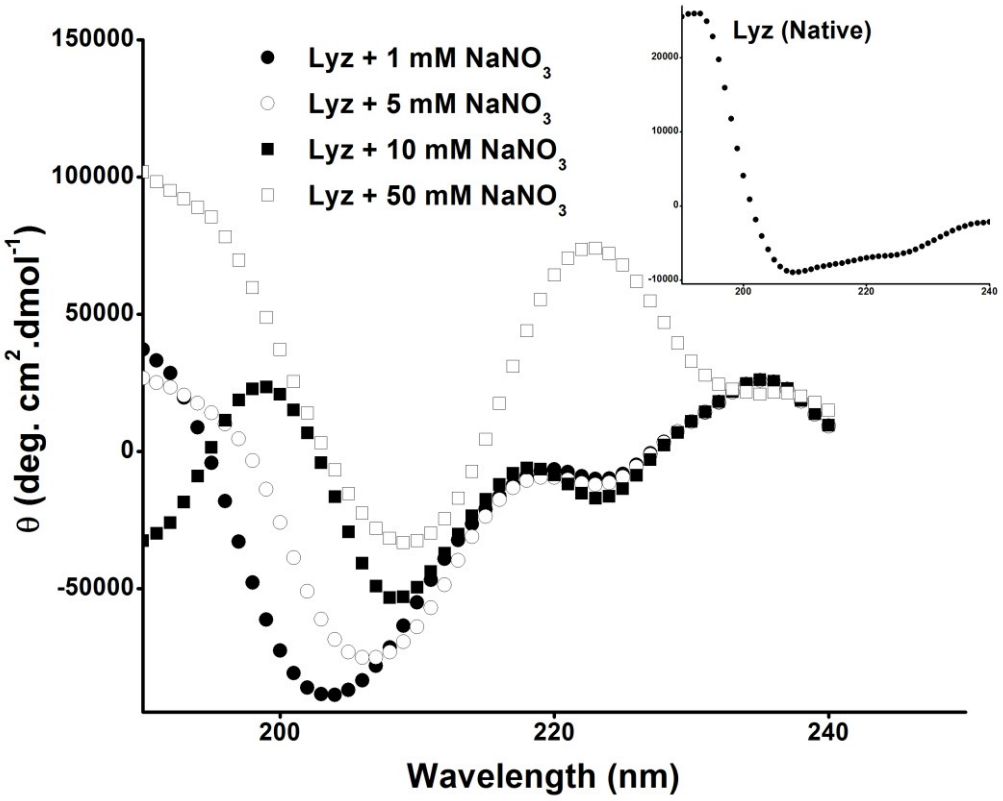

Fig. 4.

Table 1. Fluorescence Lifetimes and the population distribution of Lyz and Lyz+NO_3^- mixtures.

Sample	τ_1 (ns)	Amplitude (%)	τ_2 (ns)	Amplitude (%)
Pure Lyz	1.795±0.012	62.72	0.215±0.017	37.28
Lyz+1 mM $NaNO_3$	1.67±0.025	59.2	0.196±0.026	38.36
Lyz+5 mM $NaNO_3$	1.702±0.019	65.81	0.246±0.029	34.19
Lyz+10 mM $NaNO_3$	1.511±0.025	56.85	0.146±0.023	43.15
Lyz+50 mM $NaNO_3$	1.518±0.011	67.46	0.199±0.023	32.54

Table 2. % secondary structure of Lyz and Lyz+NO_3^- mixtures,

Sample	α-helix	β-sheet	β-turn	Unordered
Pure Lyz	25.6	30.4	13.9	30
Lyz+1 mM $NaNO_3$	19.1	15.6	31.8	33.4
Lyz+5 mM $NaNO_3$	6.6	22	64.8	6.6
Lyz+10 mM $NaNO_3$	0	57.6	22.3	20.1
Lyz+50 mM $NaNO_3$	0.7	83	2.7	13.6

Table of contents

Graphical Abstract

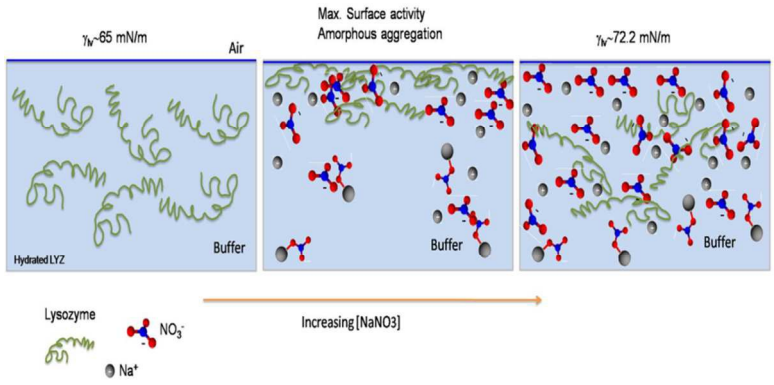

Jones Ray effect in lysozyme-sodium nitrate interface

Novelty

Interfacial rheology confirms Jones-Ray effect resulting from a synergy between lysozyme and $NaNO_3$ at air/fluid interface